Dynamic Effects of Mutations Within Two Loops of Cytochrome c_{551} From *Pseudomonas aeruginosa*

Marc Antoine Ceruso,* Alessandro Grottesi, and Alfredo Di Nola
Department of Chemistry, University of Rome "La Sapienza," Rome, Italy

ABSTRACT **In this work, we investigated the structural and dynamic consequences of two substitutions, P58A and G36P, located in two different solvent-exposed loops of cytochrome c_{551}. The results show that both mutations affect regions that are distant from the site of mutation. Here, the two loops appear to be dynamically coupled to each other, because the substitution at one site affects the structure and the dynamics of the other site. However, the substitutions at Gly-36 and Pro-58 presented substantial differences, which were related to the mechanical (rigidity and deformability) properties of the site surrounding the mutation. Although the P58A mutant conserved a significant dynamic similarity to the wild-type protein as the immediate surroundings of position 58 became more rigid, the G36P mutant, which had deformed its flexible surroundings, presented a dynamic behavior that was markedly different from that of the wild-type protein. These results suggest that perturbation of sterically isolated and flexible regions, such as solvent-exposed loops, can have strong dynamic consequences on the protein as a whole, raising the possibility that these effects could in turn affect the stability or the function of the protein. Proteins 2003;50:222–229.** © 2002 Wiley-Liss, Inc.

Key words: molecular dynamics; proline; glycine; protein function; protein stability

INTRODUCTION

Mutational changes in proteins determine a large variety of structural and functional responses. Sequence analysis of evolutionarily related proteins shows that proteins are structurally and functionally robust with respect to a plethora of amino acid changes. However, in some cases, a single-point mutation may suffice to induce dramatic structural[1–3] and functional changes[4] and to promote protein misfolding as in the case of amyloidogenic mutations.[5–8]

Previously, using the B1 domain of protein G and the repressor of primer ROP as model systems, we focused on the study of the structural and dynamic effects of mutations within rigid elements of regular secondary structure.[9,10] The results showed that the effects of surface and core mutations within rigid elements of regular secondary structure are mostly delocalized away from the point of mutation, which remains unaffected, and absorbed at specific flexible regions or residues such as loops or glycines. These findings were recently confirmed by the analysis of point mutations in a series of proteins on the basis of X-ray crystallography[11] and by molecular dynamics (MD) simulations.[12,13] The results[9,10] also suggested that the mechanical and dynamic responses of the mutant constructs are directly related to the equilibrium dynamics of the native protein. This conclusion is akin to the recently "redistribution of preexisting populations" mechanism, which has been proposed in relation to ligand-binding processes.[14,15] This analogy of effects is not surprising because both the binding of a ligand and the mutation of an amino acid introduce a perturbation of the native environment.

Here, we investigate the structural and dynamic consequences of a Pro to Ala (P58A) and a Gly to Pro (G36P) substitutions within two distinct loops of cytochrome c_{551} from *Pseudomonas aeruginosa* (Fig. 1). Both Pro-58 and Gly-36 have little interaction with their protein surroundings and lie within segments that, according to our previous results, tend to absorb the effects of mutational changes. Pro-58 lies on the surface of the protein within a non-hydrogen-bonded loop and is not linked by hydrogen-bonding, packing, or ionic interactions to the rest of the protein. However, the loop containing Pro-58 is functionally important because it carries Met-61, one of the two axial heme ligands. Gly-36 is also solvent exposed and is located (according to X-ray temperature factors) in a flexible turn that joins the second and third helix of cytochrome c_{551}. P58A (but not G36P) has been studied experimentally.[16] The effects of P58A are structurally intriguing because it has the potential to increase the flexibility of the relatively unstructured loop in which it is located, but simultaneously it does not affect the local structure of the loop because the coordination between the heme moiety and the neighboring Met-61 remains as stable as in the native structure.[16] This is remarkable because Met-61 is the weakest (toward chemical denaturation) of the two axial heme ligands,[17] and the cognate loop in mammalian cytochromes is the most unstable region of the protein.[18]

Grant sponsor: European Community Training and Mobility of Researchers Program; Grant sponsor: MURST 99 "Structural Biology of Redox Protein."

*Corrrespondence to: Marc A. Ceruso, Department of Physiology and Biophysics, Mount Siani School of Medicine, One Gustave L. Levy Place, New York, NY 10029. E-mail: mceruso@physbio.mssm.edu

Received 11 December 2001; Accepted 10 July 2002

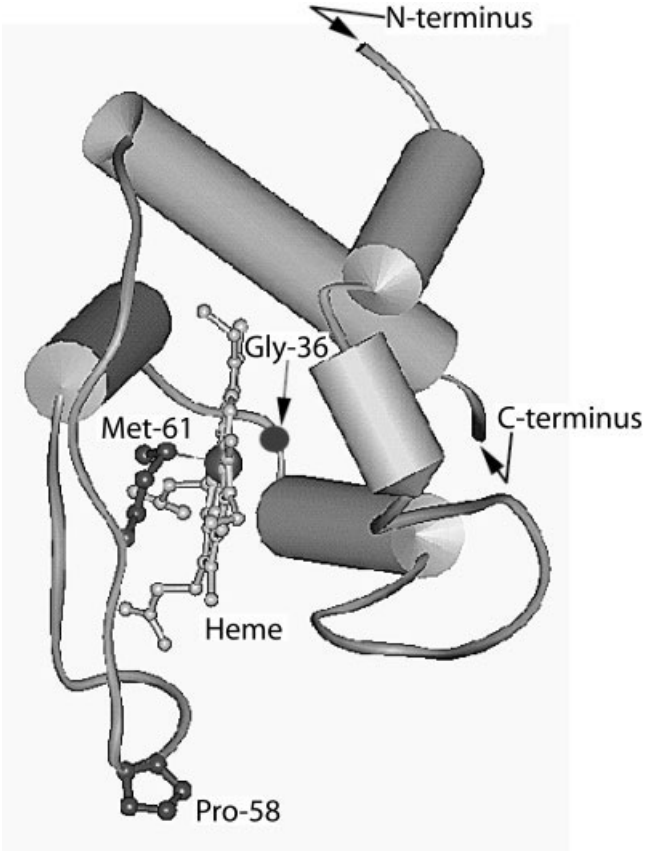

Fig. 1. Cartoon representation of cytochrome c_{551}. Cytochrome c_{551} is a globular protein consisting of four α-helices (residues ~3–10, ~27–34, ~40–50, ~68–80) and a short 3_{10} helix (~12–15). Helical sections (α and 3_{10}) are drawn as cylinders, turn and coil segments are drawn as tubes, and a ball-and-stick representation is used for the heme group. The sites of mutation Pro-58 and Gly-36, as well as the Met-61 axial heme-ligand are indicated explicitly.

Five different systems were simulated by MD. In addition to the P58A and G36P mutant systems termed P58A-C551 and G36P-C551, respectively, two independent wild-type simulations (WT1-C551 and WT2-C551) were compared structurally and dynamically to obtain a threshold of significance for the evaluation of the differences arising from mutations. Finally a "reconstituted" wild-type system, termed "A58P"-C551, starting from a structure observed in the P58A-C551 simulation was used to test the reversibility of the effects seen in P58A. The results show that the P58A mutation does not affect its immediate surroundings and Met-61 in particular, in agreement with experimental observations. On the contrary, P58A affects the structure and the dynamics of a flexible region centered on Gly-36, located on the opposite side of the heme group (the C-α carbons of Gly-36 and Pro-58 are 25 Å apart). Incidentally, the mechanical coupling between the two sites is shown to correspond to an intrinsic dynamic feature of the native fold in agreement with our previous findings.[9,10]

However, despite their coupling, the substitutions at Gly-36 and Pro-58 present substantial differences. The P58A substitution increased the rigidity of the immediate loop and had the same characteristics as mutations within rigid helices and sheets (e.g., absence of local perturbation and delocalization to a distant flexible region (the turn at Gly-36). On the contrary, the G36P substitution, which was intended to deform its immediate environment, induced a dynamic behavior markedly different from that of wild type. The results indicate that the mechanical properties associated within the site of mutation play a critical role in the way the protein will respond to an amino acid substitution and suggest that mutations within solvent-exposed flexible regions, such as loops, can affect directly the global dynamic behavior of the protein.

MATERIALS AND METHODS

Systems

Five different systems were studied computationally. Three systems had native amino acid sequence and were designated by WT1-C551, WT2-C551, and "A58P"-C551. The quotes around A58P are meant to underscore that this system does not correspond to a mutant sequence. The remaining two systems were named P58A-C551 and G36P-C551 and designate mutant proteins where Pro-58 (respectively, Gly-36) has been replaced by an alanine (respectively a proline) residue. Initial coordinates for wild-type and mutant systems, except for "A58P" -C551, were taken from entry 351c[19] of the protein data bank. Coordinates for "A58P"-C551 were built from P58A-C551 after 1850.70 ps of simulation. Mutations were constructed within InsightII 97.0 (Biosym/MSI San Diego, CA).

Simulations

MD simulations were performed with Gromacs.[20] Simulations were conducted at constant temperature within a fixed-volume rectangular box by using periodic boundary conditions. All systems were simulated in the presence of explicit SPC-water molecules.[21] Each system contained ~3000 water molecules and a total of 10,000 atoms. The initial velocities were taken randomly from a Maxwellian distribution at 300 K. The two independent wild-type simulations (WT1-C551 and WT2-C551) used a different box size and a different set of initial velocities. A nonbonded cutoff of 12.0 Å was used for both Lennard-Jones and Coulomb potentials. The pair lists were updated every 10 steps. The SHAKE algorithm[22] was used to constrain bond lengths. The temperature was held constant by coupling to an external bath[23] using a coupling constant (τ = 0.002 ps) equal to the integration timestep. For all systems, WT1-C551, WT2-C551, P58A-C551, and G36P-C551, except "A58P"-C551, the solvent was relaxed by energy minimization followed by 10 ps of MD at 300 K, while restraining protein and heme atomic positions with a harmonic potential. The systems were then minimized without restraints and their temperature brought to 300 K in a stepwise manner: Ten-picosecond-long MD runs were conducted at 50, 100, 200, and 250 K before starting the production runs at 300 K. "A58P"-C551 was set up differently. After transforming Ala-58 within the P58A-C551 system back to a proline residue, the newly obtained "A58P"-C551 system was only minimized before pursuing

with MD at 300 K. All runs but that of "A58P"-C551 (1.6 ns) were at least 2.5 ns long. Average properties were computed after discarding the first 1000 ps of simulation for each system. Comparing mutant systems, including "A58P" -C551, with respect to wild-type, the two independent wild-type simulations were merged because their average properties were statistically identical (see Results), and comparisons were made with respect to this "merged" system called WT-C551.

Dynamic Signatures and Convergence

Dynamic signature

Quantitative characterization of the dynamic properties of each system relied on principal component analysis of the covariance matrix of the positional fluctuations of the C-α atoms, as described previously.[24–26] This matrix was built from the equilibrated portion of the trajectories (beyond the first nanosecond), and its diagonalization afforded the principal directions of the large-amplitude concerted motions (principal eigenvectors), which characterize the essential subspace of a protein's internal dynamics. The dynamic signature of a protein was defined by the subspace corresponding to the first 10 eigenvectors with largest eigenvalues of the covariance matrix of the fluctuations. Comparison of the dynamic properties of two proteins involved taking the mean-square inner product, *MSIP*, between the corresponding dynamic signatures (first 10 eigenvectors):

$$MSIP = \left(\frac{1}{10} \sum_{i=1}^{10} \sum_{j=1}^{10} (\eta_i^a \, \eta_j^b)^2 \right) \quad (1)$$

where η_i^a and η_j^b are respectively the ith and jth eigenvectors from set "a" (first protein) and set "b" (second protein).

Convergence of dynamic signatures

The convergence/divergence of the MSIPof a given protein system with respect to the equilibrium dynamic signature of a reference system involved the following steps: the trajectory of the tested system was subdivided into segments of increasing length, each segment being 50 ps longer than the previous one. Then, the (partial) dynamic signature of each segment was computed and compared to the dynamic signature of the reference system (derived from the entire equilibrated trajectory) by calculating the MSIP between the corresponding eigenvector sets. To establish the significance of these values, the probability density of the total squared-projection value of one vector onto a set of orthogonal vectors was computed as described previously.[27] This probability depends on the total dimensionality of the space under consideration, here 3×82 (C-α atoms) = 246. A vector in a 246-dimensional space, taken randomly, would have a 1% probability to have a total squared-projection value > 0.076 when projected onto a 10-dimensional orthonormal basis set; this reference value was designated by $S^2_{0.99}$.

RESULTS

Wild-Type Systems

To provide reference thresholds for the comparison of the structural and dynamic properties between wild-type and mutant systems, two independent simulations of the wild-type protein, WT1-C551 and WT2-C551, were performed starting from the coordinates deposited in entry 351c of the protein data bank.[19] To determine the location and the degree of conformational differences between WT1-C551 and WT2-C551, for each simulation, the root-mean-square deviation (RMSD) per residue was calculated for the average structure of the other simulation, and the mean value between the two simulations was computed [Fig. 2(A), filled circles]. Besides some large differences regarding the last two residues (81–82) and some small differences (≤1.5 Å) within other (the N-terminus, and residues 36–39 and 54–58) flexible regions [Fig. 2(B)], most residues had an RMSD difference smaller than 1.0 A. This finding indicates that the structural behavior of the two simulations was very similar, as also suggested by the observation that their solvent accessible surface area, radius of gyration, and secondary structure content were all statistically indistinguishable (data not shown). WT1-C551 and WT2-C551 also conserved the structural properties of the original X-ray structure, with the differences being confined to the flexible segments of the protein (data not shown).

The similarity of the dynamic properties of WT1-C551 and WT2-C551 was evaluated by calculating the overlap between their corresponding dynamic signatures (see Materials and Methods). The time evolution of the *MSIP* of each wild-type system was calculated for the other wild-type system, and the average was taken at each point [Fig. 3(A)]. The dynamic overlap between the two simulations reached the significant value of 0.40 (>5 times the value that could be expected by chance with a 1% probability: $S^2_{0.99} = 0.076$; see Materials and Methods) after 250 ps of simulation and grew up to a value of 0.64 after 2.5 ns of simulation, confirming that the two simulations had a comparable dynamic behavior and that the time length of the simulations was sufficient to achieve a meaningful description of the dynamic signature of each system.[27] For comparison purposes, the MSIP between the present set of eigenvectors and a set obtained from an MD simulation of an unrelated protein (myoglobin) but which is also α-helical is only 0.16. Thus, the *MSIP* = 0.64 is highly significant, and its value represents an upper boundary reference for the comparison of wild-type and mutant simulations.

In conclusion, the two wild-type simulations were structurally and dynamically similar, and reference thresholds for the structural and dynamic comparison of mutant and wild-type systems have been set. In addition, the length of the simulation was shown to be sufficient to achieve a meaningful description of wild-type dynamic properties. In what follows, wild-type properties correspond to those derived from the combination of the equilibrated segments (beyond the first nanosecond) of the two independent trajectories (WT-C551).

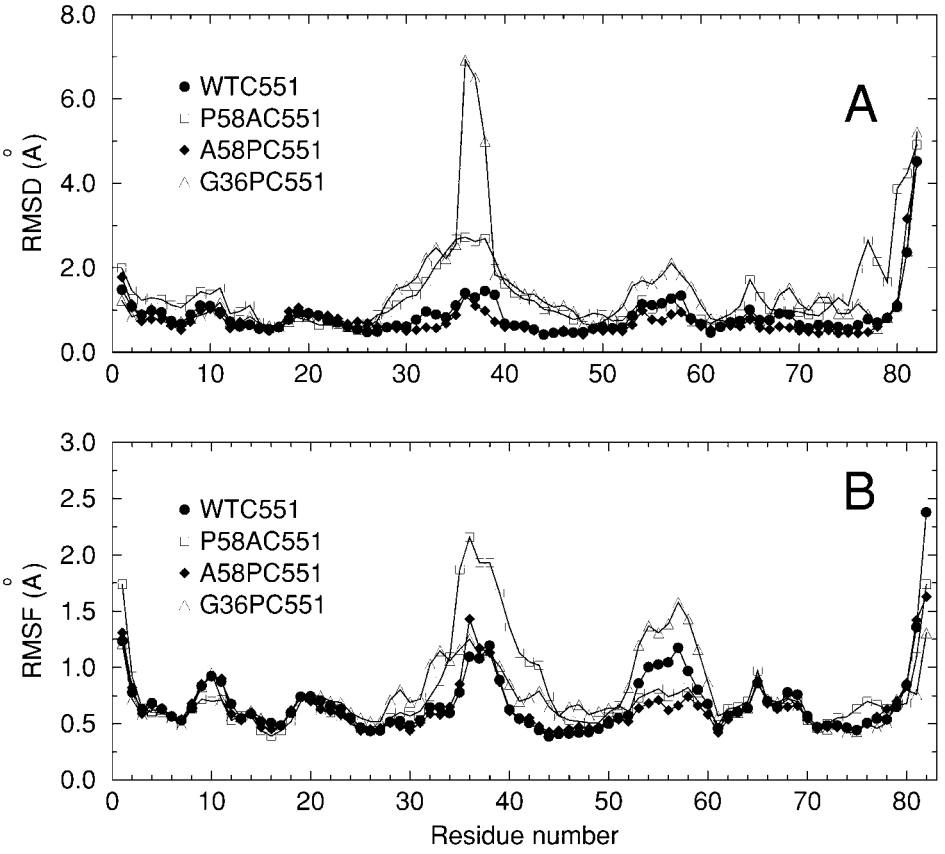

Fig. 2. Backbone root-mean-square deviation (RMSD) and fluctuation (RMSF). **A:** RMSD with respect to the average WT-C551 configuration: P58A-C551 (open squares), "A58P"-C551 (filled diamonds), and G36P-C551 (open triangles). The mean of the RMSD of WT1-C551 and WT2-C551 with respect to the average structure of WT2-C551 and WT1-C551 is represented by filled circles. **B:** RMSF: same coding as above; here the filled circles represent the fluctuations of the merged system WT-C551, not an average of WT1-C551 and WT2-C551.

Effects of Pro-58 to Ala-58 Mutation

P58A did not have a significant structural impact on its immediate surroundings as evidenced by the comparison of the local RMSD [Fig. 2(A)] and backbone ϕ/ψ dihedral torsions (data not shown) between P58A-C551 and WT-C551. Similarly, P58A did not affect the overall structure of cytochrome c_{551} in a significant manner (Table I). The structural effects of the P58A mutation were concentrated within two amino acid segments spatially distant from the site of mutation [Fig. 2(A), open squares] and surrounding Gly-36. The first segment extended itself from residue 32 to residue 40, encompassing the end of the second α-helix (residues 27–34), the following turn (residues 36–39), and the third α-helix (residues 40–50). This segment lies diagonally opposite from position 58 on the other side of the heme-plane. The second segment stretched itself from residues 76–81 and corresponds to the C-terminal helix. This helix is located right "above" Gly-36. Residues in the N-terminal helix and Ala-65 were also perturbed, but to a lesser extent.

Dynamically, only one of the above segments (residues 34–43) had larger fluctuations with respect to WT-C551 [Figs. 2(B) and 4 open squares], whereas the site of mutation remained unaffected (RMSF $\leq$1.0 Å). It is interesting to note that the regions surrounding positions 58 and 36 were already dynamically coupled to each other in the wild-type simulations. This result is suggested by the observation that both regions carried the highest components on the first principal eigenvector in the native simulations (Fig. 4 filled circles). Because these are long-range correlations and the simulations used a cutoff-based treatment of the electrostatic interactions that could result in long-range artifacts, we also performed a 2.5-ns simulation of the wild-type system using the PME method for the treatment of electrostatic interactions. Essential dynamics analysis of the latter simulation showed that the dynamic correlation between the two loops was also present in the PME simulations (data not shown).

Reversibility and Reciprocity: "A58P"-C551 and G36P-C551

If the effects observed for the P58A mutant reflect intrinsic equilibrium properties of the native fold, they should be reciprocal and reversible. To test the reversibility of the effects, Ala-58 in P58A-C551 was transformed back into a proline, effectively regenerating a wild-type

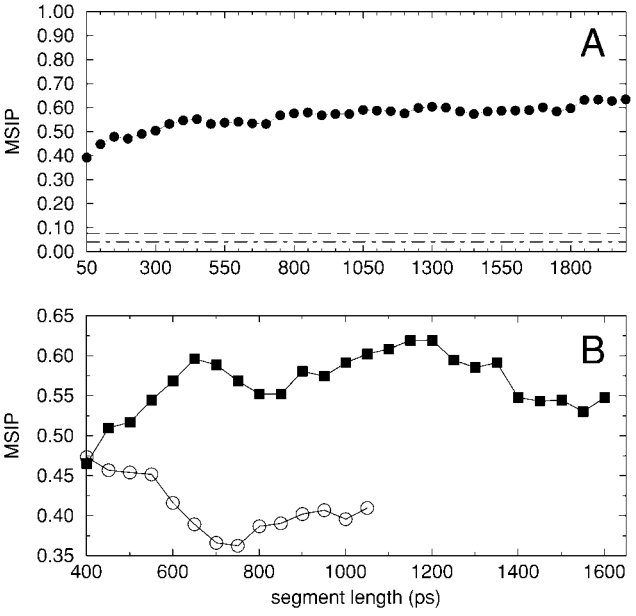

Fig. 3. Convergence and divergence of dynamic signatures. The abscissa report the time length of the trajectory segment used to define the (partial) dynamic signature of the tested system. **A:** Time evolution of the average *MSIP* for WT1-C551 and WT2-C551 for the dynamic signatures of WT2-C551 and WT1-C551. The dot-dashed line represents the mean value of the expected random squared-projection S^2, the long-dashed line reports the value of $S^2_{0.99} = 0.076$ (see Materials and Methods). **B:** Time evolution of the *MSIP* of "A58P"-C551 with respect to WT-C551 (filled squares) and of the *MSIP* of P58A-C551 with respect to WT-C551 (open circles).

sequence, and the new system was termed "A58P"-C551. The initial coordinates for this system were those of P58A-C551 after 1850.70 ps. This choice corresponded to a system with an intermediate RMSD value of 1.47 Å (RMSDs ranged from 1.02 to 2.09 Å for the average wild-type configuration).

Confirming the reversibility of the effects, "A58P"-C551 recovered most of its wild-type structural properties, such as R_G, helical content, and HB4 hydrogen-bonding (Tables I and II). The average RMSD of "A58P"-C551 for the average wild-type configuration (1.12 ± 0.14 Å) was comparable to the one between the two independent wild-type simulations (0.99 ± 0.16). In the same manner, the mechanical and dynamic properties of "A58P"-C551 became more native like, while diverging from those of P58A-C551 [Fig. 3(B)]. The *MSIP* = 0.61 between the dynamic signatures of "A58P"-C551 and WT-C551 was almost indistinguishable from the one (*MSIP* = 0.64) between the two independent wild-type simulations (Table III), and the atomic correlation along the first eigenvector of "A58P"-C551 resumed most of the wild-type features [Fig. 4(B)].

To test the reciprocity of the effects seen in P58A-C551, Gly-36, which had been the principal residue affected by the P58A substitution, was replaced by a proline residue. The choice of the proline was meant to offer the largest mechanical contrast with the glycine by forcing the local backbone dihedral angle at position 36 to adopt a value (~ -60 degrees) different from that of the Gly-36 in the native structure (~ -132 degrees). The new system was termed G36P-C551. The conformational and dynamic features of the G36P-C551 system confirmed the reciprocity of the mechanical link between positions 58 and 36, because its RMSD and RMSF values (Fig. 2 open triangles), as well as the components of its first eigenvector (Fig. 4 open triangles) clearly showed that the G36P substitution perturbed the 53–59 region of the protein.

Effects of Gly-36 to Pro-36 Mutation

The other purpose of the G36P substitution was to evaluate the effects of a mutation within another loop, which is typically used for absorbing the effects of mutations.[9,10,28] In this respect, the G36P mutant presented two features that were particularly noteworthy and that distinguished it from the P58A mutant. First and as intended, the G36P mutation induced significant conformational changes in its immediate surroundings, as suggested by the large RMSD of the region immediately surrounding the Gly/Pro-36 [Fig. 2(A) open triangles]. This was in marked contrast with P58A, which not only had maintained the structural integrity of its local environment but had reinforced its rigidity as well. Second, the dynamic behavior of G36P-C551 (unlike that of P58A-C551) was significantly different from that of the wild-type system. This was suggested by the very low *MSIP* value between the dynamic signatures of the G36P and wild-type systems (*MSIP* = 0.20, Table III). Note that this value is close to that obtained when comparing the dynamic signatures of WT-C551 with that of an unrelated protein such as myoglobin (*MSIP* = 0.16). This indicates that G36P-C551 had lost almost all the dynamic characteristics of cytochrome c_{551}, in contrast to P58A-C551, which had maintained significant similarity with the wild-type system (*MSIP* = 0.52, Table III).

DISCUSSION AND CONCLUSION

In the present MD study of cytochrome c_{551}, we have investigated the structural and dynamic consequences of a Pro to Ala (P58A-C551) and Gly to Pro (G36P-C551) substitution, each located in a solvent-exposed loop. The significance of the differences in the dynamic properties between the various mutant and wild-type constructs was established by using two independent wild-type simulations to define reference thresholds for the corresponding dynamic properties. It was also established that all simulations were sufficiently long to achieve a significant description of the dynamic properties of each system. This work complements our previous studies, which had focused on amino acid substitutions within regular elements of secondary structure.[9,10]

Comparative analysis of the MD simulations of wild-type and mutant constructs showed the existence of a mechanical link between the regions surrounding Pro-58 and Gly-36, because the perturbation of Gly-36 (G36P-C551) affected the Pro-58 containing loop, and the perturbation of Pro-58 (in P58A-C551) reciprocally perturbed the turn associated with Gly-36. It is noteworthy that McCammon and coworkers also found a strong correlation peak in

TABLE I. Structural Statistics[†]

	WT-C551	P58A-C551	"A58P"-C551	G36P-C551
SASA (Å^2)	5114 (116)	5249 (118)	5223 (88.0)	5228 (119)
R_G (Å)	11.4 (0.1)	11.8 (0.1)	11.4 (0.1)	11.7 (0.1)
$RMSD_{XRAY}$ (Å)	1.50 (0.23)	1.72 (0.18)	1.76 (0.20)	1.82 (0.27)
Alpha	42.0 (2.2)	38.6 (2.3)	41.9 (1.8)	39.4 (2.1)
Turn	18.8 (1.8)	19.3 (2.3)	18.2 (1.3)	20.0 (1.7)
Coil	19.9 (1.6)	23.0 (2.1)	21.0 (0.9)	20.8 (1.7)
HBO	55.2 (2.5)	52.9 (2.7)	53.7 (2.4)	55.1 (2.6)
HB4	32.8 (1.4)	28.5 (1.9)	32.4 (1.1)	31.5 (1.0)
HB3	7.7 (2.2)	8.6 (2.3)	7.3 (2.1)	6.7 (1.9)
HB2	4.6 (1.5)	6.1 (1.6)	4.3 (1.3)	6.3 (1.8)

[†]Solvent accessible surface area (SASA), radius of gyration (R_G), and average backbone root-mean-square deviation with respect to the X-ray coordinates ($RMSD_{XRAY}$). Total number of residues in alpha-helical (Alpha), turn (Turn), and coil (Coil) conformation. HBO: total number of hydrogen bonds, and HB4,3,2: total number of hydrogen bonds of type $O_i \leftarrow HN_{i+4,3,2}$. SDs are given in parentheses.

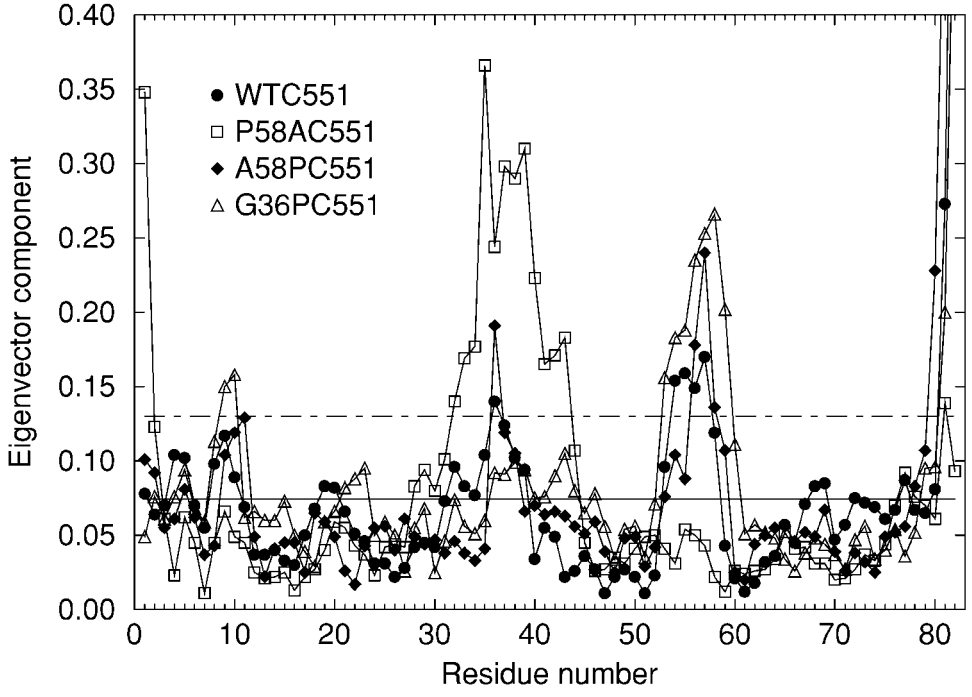

Fig. 4. Atomic components of the first eigenvector in WT-C551 (filled circles), P58A-C551 (open squares), A58P-C551 (filled diamonds), and G36P-C551 (open triangles). Graph representation of the components: after having excluded the last two residues (which carry disproportionately large component values), significantly large components were detected above the 2 SD cutoff (dot-dashed line), and the solid line represents the mean value.

the atomic correlation matrix between the cognate segments in their MD simulation of cytochrome c,[29] further supporting the idea that, as shown by the present results, the coupling between the two loop segments corresponds to an intrinsic mechanical feature of the native (cytochrome c_{551}) fold. This finding is also in agreement with our previous studies[9] showing that mutational effects develop about the fold-intrinsic mechanics of the native protein instead of inducing new mechanical features. Note that this corresponds to a redistribution of the native conformational ensemble on mutation, a mechanism that was recently confirmed through comparative analysis of the X-ray structures of a series of proteins for which a large number of mutants were also solved structurally.[11]

Despite their intrinsic coupling, the substitutions at Gly-36 and Pro-58 presented substantial dynamic differences. These differences were associated with the mechanical properties of their immediate environment. Indeed, structurally and in agreement with experimental observations, P58A-C551 showed that the immediate surroundings of the site of mutation, and the iron/Met-61 coordination in particular, were not affected by the substitution of

TABLE II. Structural Cross-Comparison of Systems[†]

	Average structures			
Systems	WT-C551	P58A-C551	"A58P"-C551	G36P-C551
WT-C551	0.99 (0.16)	1.45 (0.18)	1.09 (0.18)	1.58 (0.14)
P58A-C551	1.51 (0.20)	0.88 (0.14)	1.74 (0.18)	1.47 (0.19)
"A58P"-C551	1.12 (0.14)	1.83 (0.22)	0.71 (0.09)	1.68 (0.15)
G36P-C551	1.78 (0.15)	1.77 (0.17)	2.06 (0.14)	0.80 (0.12)

[†]Backbone RMSD (Å) of each system relative to their own and other systems' average configuration. SDs are given in parentheses.

TABLE III. *MSIP* Values Between Dynamic Signatures

	WT-C551	P58A-C551	"A58P"-C551	G36P-C551
WT-C551	0.64[a]	0.5	0.61	0.2
P58A-C551		—	0.46	0.23
"A58P"-C551			—	0.18
G36P-C551				—

[a]This is the *MSIP* value between the two independent wild-type simulations.

Pro-58. This was the case because P58A resulted in an increase of the rigidity of the 52–61 hairpin loop as measured by the RMSF [Fig. 2(B)]. In contrast, G36P strongly deformed its immediate and flexible environment (Fig. 2). Consequently, although P58A-C551 was dynamically comparable to the wild -type simulations (Table III), the G36P substitution induced a dynamic behavior markedly different from that of wild-type (Table III), indicating that perturbation of a solvent-exposed flexible region, such as the loop containing Gly-36, can have marked effects on the dynamic properties of the protein as a whole. From these results, it is interesting to speculate that these mechano-dynamic changes could in turn affect the stability or the function of the protein. This speculation seems supported by the role that some turn/loop amino acids play in the structural and functional integrity of proteins. For example, in the case of the homodimeric 4-helix-bundle ROP, perturbation of the loop joining the helices of the monomer leads to dramatic rearrangements in the quaternary structure of the protein.[2,30] And more recently, the dynamic and functional coupling between the SH2 and SH3 domains of c-Src and Hck was directly linked to the mechanical properties of the linker between these two domains.[31]

ACKNOWLEDGMENTS

We thank Carlo Travaglini-Allocatelli and Francesca Cuttruzolà for helpful and stimulating discussions.

REFERENCES

1. Matthews JM, Norton RS, Hammacher A, Simpson RJ. The single mutation phe173→ala induces a molten globule-like state in murine interleukin-6. Biochemistry 2000;39:1942–1950.
2. Glykos NM, Cesareni G, Kokkinidis M. Protein plasticity to the extreme: changing the topology of a 4-α-helical bundle with a single amino acid substitution. Structure 1999;7:597–603.
3. Consonni R, Sintomo L, Fusi P, Tortora P, Zetta L. A single-point mutation in the extreme heat- and pressure-resistant Sso7d protein from *Sulfolobus solfataricus* leads to a major rearrangement of the hydrophobic core. Biochemistry 1999;38:12709–12717.
4. Ingram VM. Gene mutation in human haemoglobin: the chemical difference between normal and sickle cell haemoglobin. Nature 1957;180:326–328.
5. Kelly JW. Amyloid fibril formation and protein misassembly: a structural quest for insights into amyloid and prion diseases. Structure 1997;5:595–600.
6. Booth DR, Sunde M, Bellotti V, Robinson CV, Hutchinson WL, Fraser PE, Hawkins PN, Dobson CM, Radford SE, Blake CCF, Pepys MB. Instability, unfolding and aggregation of human lysozyme variants underlying amyloid fibrillogenesis. Nature 1997;385:787–793.
7. Carrel RW, Gooptu B. Conformational changes and disease—serpins, prions and Alzheimer's. Curr Opin Struct Biol 1998;8:799–809.
8. Morozova-Roche LA, Zurdo J, Spencer A, Noppe W, Receveur V, Archer DB, Joniau M, Dobson CM. Amyloid fibril formation and seeding by wild-type human lysozyme and its disease-related mutational variants. J Struct Biol 2000;130:339–351.
9. Ceruso MA, Amadei A, Di Nola A. Mechanics and dynamics of B1 domain of protein G: role of packing and surface hydrophobic residues. Protein Sci. 1999;8:147–160.
10. Ceruso MA, Grottesi A, Di Nola A. Effects of core-packing on the structure, function and mechanics of a four-helix-bundle protein ROP. Proteins 1999;36:436–446.
11. Sinha N, Nussinov R. Point mutations and sequence variability in proteins: redistribution of preexisting populations. Proc Natl Acad Sci USA 2001;98:3139–3144.
12. Falconi M, Stroppolo ME, Cioni P, Strambini G, Sergi A, Ferrario M, Desideri A. Dynamics-function correlation in Cu,Zn superoxide dismutase: a spectroscopic and molecular dynamics simulation study. Biophys J 2001;80:2556–2567.
13. Ota N, Agard DA. Enzyme specificity under dynamic control II: principal component analysis of α-lytic protease using global and local solvent boundary conditions. Protein Sci 2001;10:1403–1414.
14. Freire E. The propagation of binding interactions to remote sites in proteins: analysis of the binding of the monoclonal antibody D1.3 to lysozyme. Proc Natl Acad Sci USA 1999;96:10118–10122.
15. Kumar S, Ma B, Tsai CJ, Sinha N, Nussinov R. Folding and binding cascades: dynamic landscapes and population shifts. Protein Sci 2000;9:10–19.
16. Bigotti MG, Travaglini-Allocatelli C, Stainforth RA, Arese M, Cutruzzolà F, Brunori M. Equilibrium unfolding of a small bacterial cytochrome, cytochrome c_{551} from *Pseudomonas aeruginosa*. FEBS Lett 1998;425:385–390.
17. Hamada D, Kuroda Y, Kataoka M, Aimoto S, Yoshimura T, Goto Y. Role of heme axial ligands in the conformational stability of the native and molten globule states of horse cytochrome *c*. J Mol Biol 1996;256:172–186.
18. Bai Y, Sosnick TR, Mayne L, Englander SW. Protein folding intermediates: native-state hydrogen exchange. Science 1995;269:192–197.
19. Matsuura Y, Takano T, Dickerson RE. Structure of cytochrome c_{551} from *Pseudomonas aeruginosa* refined at 1.6 Å resolution and comparison of the two redox forms. J Mol Biol 1982;156:389–409.
20. Berendsen HJC, van der Spoel D, van Drunen R. Gromacs: a message-passing parallel molecular dynamics implementation. Comp Phys Comm 1995;95:43–56.
21. Berendsen HJC, Postma JPM, Van Gunsteren WF, Hermans J. Interaction models for water in relation to protein hydration. In:

Pullman B, editor. Intermolecular forces. Dordrecht: D. Reidel Publishing Company; 1981. p 331–342.
22. Ryckaert JP, Ciccotti G, Berendsen HJC. Numerical integration of the cartesian equations of motion of a system with constraints: molecular dynamics of n-alkanes. J Comp Phys 1977;23:327–341.
23. Berendsen HJC, Postma JPM, Di Nola A, Haak JR. Molecular dynamics with coupling to an external bath. J Chem Phys 1984;81:3684–3690.
24. Garcia AE. Large-amplitude nonlinear motions in proteins. Phys Rev Lett 1992;68:2696–2699.
25. Wong CF, Zheng C, Shen J, McCammon A, Wolynes PG. Cytochrome C: a molecular proving ground for computer simulations. J Phys Chem 1993;97:3100–3110.
26. Amadei A, Linssen ABM, Berendsen HJC. Essential dynamics of proteins. Proteins 1993;17:412–425.
27. Amadei A, Ceruso MA, Di Nola A. On the convergence of the conformational coordinates basis set obtained by essential dynamics analysis of proteins' molecular dynamics simulations. Proteins 1999;36:419–424.
28. Spiller B, Gershenson A, Arnold FH, Stevense RC. A structural view of evolutionary divergence. Proc Natl Acad Sci USA 1999;96: 12305–12310.
29. McCammon JA, Harvey SC. Dynamics of proteins and nucleic acids. New York: Cambridge Unversity Press; 1987.
30. Lassalle MW, Hinz HJ, Wenzel H, Vlassi M, Kokkinidis M, Cesareni G. Dimer-to-tetramer transformation: loop excision dramatically alters structure and stability of the ROP four-helix bundle protein. J Mol Biol 1998;279:987–1000.
31. Young MA, Gonfloni S, Superti-Furga G, Roux B, Kuriyan J. Dynamic coupling between the SH2 and SH3 domains of a c-Src and Hck underlies their inactivation by C-terminal tyrosine phosphorylation. Cell 2001;105:115–126.